H. C. Thomas, 8442

The University of Alabama in Birmingham
School of Engineering
Department of Mechanical and Materials Engineering
205/934-5406

FROM : Clemson University
School of Engineering
Clemson, S.C.

TITLE : Final Report

DATE : September 17, 1981

CONTRACT : NAS8 - 33805: Further Study on the Near Solidus Intergranular Cracking of Inconel 718

AUTHOR : Raymond G. Thompson
University of Alabama in Birmingham
Department of Mechanical and Materials Engineering
University Station/Birmingham, AL 35294

PREPARED FOR : George C. Marshall Space Flight Center,
Marshall Space Flight Center, Alabama 35812

FURTHER STUDY OF NEAR SOLIDUS INTERGRANULAR CRACKING IN INCONEL 718

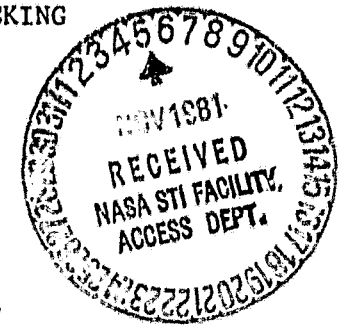

BY

Raymond G. Thompson
Assistant Professor of Materials Engineering
Formerly at Clemson University
Clemson, South Carolina
Presently at The University of Alabama in Birmingham

ABSTRACT

The cause of microfissuring in the heat affected zone of Inconel 718 welds has eluded investigators since the alloy's development in the early 1960's. Microfissuring is justifiably a primary concern at NASA/MSFC since there are a multitude of EB and TIG welded parts in the SSME. A program was initiated at MSFC to develop microfissuring envelopes which could predict the safe welding parameters for Inconel 718 to avoid microfissuring. In support of this program, a series of tests were performed to determine the strain necessary to initiate intergranular cracking in Inconel 718 as a function of temperature. These tests contained enough scatter near the melting temperature that questions remained as to the best curve or curves to fit to the data. The present research analyzed the scatter in data by fracture surface analysis. It was determined that the scatter was due to incipient melting in the grain boundary region. The melting contributed to low fracture strain but had only a small effect on the incipient cracking strain.

Gleeble tests, which could be interrupted by water quenching, were used to study the incipient intergranular melting of Inconel 718. This modified weld simulation test provided a sufficiently rapid quench to preserve the intergranular microstructure created during incipient melting. This structure was studied both microscopically and with energy dispensive

x-ray analysis. The present report discusses the implications of incipient melting and low-strain incipient cracking on the development of microfissuring envelopes.

INTRODUCTION

The development of useful microfissuring envelopes which predict microfissuring events in terms of welding parameters is a difficult, but worthwhile task. Given a microfissuring envelope for a certain metal, the welding machine can be programed to maximize efficiency while minimizing the risk of producing weld defects. In order to develop a microfissuring envelope, the mechanical response of the metal during the welding cycle must be known. More precisely, the strain necessary to initiate intergranular cracks at temperatures characteristic of the welding cycle must be known.

Previous work[1] has shown that the strain necessary to initiate intergranular cracking near the solidus temperature of Inconel 718 is nearly constant at about 0.1 percent plastic strain. Although the incipient-cracking strain is about constant, the fracture strain varies widely between about 0.1% and 26.0% plastic strain. The fact that fracture strain is not an indication of incipient-crack strain is important because the presently accepted method for determining microfissure sensitivity is the percent reduction in area at fracture (%RA). The %RA data in the literature cannot be used in the calculation of a microfissuring envelope due to the obvious difference found between incipient-crack strain and fracture strain.

Not only cannot the %RA data be used in calculating a microfissuring envelope, but neither can the incipient-crack strain developed in the previous study be used. The incipient-crack strain cannot be used due to the on-heating, on-cooling nature of the welding thermal cycle. The hot tensile test[1] used to make incipient-crack strain measurements is unlike the hot ductility test [2,3] used to make %RA measurements. The hot ductility test simulates a welding thermal cycle and fracture tests are made during

both the on-heating and on-cooling portions of the thermal cycle.[2,3] Figure 1 shows that the mechanical response of the metal has a much different temperature sensitivity on cooling than on heating. The hot tensile test only measures the mechanical response on heating. Since microfissures form due to thermal contraction strain during cooling, it is evident that incipient-crack strain, on cooling, should be used in the calculation of microfissuring envelopes.

The present paper presents experimental evidence which suggests a method for estimating the on-cooling, incipient-crack strain. The method combines the on-cooling temperature sensitivity data from hot ductility tests with the incipient-crack strain from hot tensile test.[2,3] This gives an estimate of the on-cooling temperature sensitivity of the incipient-crack strain to be used in calculating microfissuring envelopes for Inconel 718.

EXPERIMENTAL PROCEDURE AND RESULTS

Fracture Surface Analysis

Fractographic analysis was performed on the hot tensile test specimens given below:

Specimen Number	Test Temperature (F)	Fracture Strain	Incipient-Crack Strain
13	2150	26%	0.1
14	2175	11	0.1
4	2200	0	0.1
9	2200	3	0.1
15	2200	0.7	0.1
10	2300	0	0
2	2350	4.5	4.5
11	2350	3	3
12	2350	-	-

TABLE I

The specimen fracture surface was prepared for observation by the following cleaning steps:

1. ultrasonic cleaning in alcohol
2. stripping of the fracture surface with replica tape
3. ultrasonic cleaning in acetone
4. wash in alcohol

The fracture surfaces thus prepared were examined using a scanning electron microscope. Typical fracture surface appearances are shown in Figures 2-13 of Appendix A. The reader is referred elsewhere[1] for details of the hot tensile test and incipient-crack strain calculation.

Interrupted Gleeble Test

The interrupted Gleeble test consists of rapidly quenching specimens from various temperatures during the thermal cycle experienced by the HAZ. This was done in order to follow the progressive change of intergranular microstructure in the HAZ during welding. A model 510 Gleeble machine was programmed to simulate the thermal cycle of a HAZ for arc-welded, 1/2 inch stainless steel plate. This material was chosen because of existing data which allowed the calculation of the desired thermal cycle. The HAZ

thermal cycle for an Inconel alloy should be very similar to that for stainless steel. The typical thermal cycle imposed on the specimens is shown in Figure 14.

The specimens were quenched from various temperatures during the thermal cycles by two methods used simultaneously. Water cooled copper grips extracted heat from both ends of the specimen while room temperature tap water was poured directly on the specimen surface. This produced surface quench rates of several thousand degrees F per second. The thermal cycles and quench rates were recorded with surface mounted thermocouples and a high speed oscillograph recorder. Typical interrupted thermal cycles are shown in Figure 14.

Reflected light metallography was used to study the evolution of intergranular microstructure during the HAZ thermal cycle. A typical evolution of Inconel 718, HAZ microstructure is shown in Figure 15. This evolution of microstructure was similar for both the solution annealed and fully heat treated conditions (Table II).

Solution Annealed	Fully Heat Treated
1750 F for 1 hour	Solution Anneal
Furnace Cool	plus
(in vacuum)	1400F for 8 hours
	Furnace cool to 1200F
	1200F for 10 hours
	Furnace Cool
	(in vacuum)

TABLE II

EDAX analysis of the microstructure showed that second phases, containing about 47 w/o (Nb + Mo), melted on heating and wet the grain boundaries. This enriched the grain boundaries to a (Nb + Mo) content of 28 w/o (Figure 16). These enriched grain boundaries solidified over a temperature range of several hundred degrees on cooling, thus severely depressing the solidus temperature on cooling. The incipient melting of

the (Nb + Mo) enriched phase on heating was verified by differential thermal analysis (DTA) as seen in Figure 17. The solidus of the (Nb + Mo) enriched grain boundaries on cooling could not be detected by DTA which indicates a very broad solidification temperature range.

DISCUSSION

The following discussion is aimed at showing cause for revising earlier experimental data so that such data can be used to calculate more accurate microfissuring envelopes. The revisions are based on new experimental evidence as discussed below.

Figure 18 shows an experimental relationship between plastic strain, both incipient-crack and fracture, and temperature for Inconel 718. This data is for the on-heating portion of the HAZ thermal cycle. The incipient-crack strain data contained scatter at 2200F such that the author was undecided as to drawing a single-nosed or double-nosed curve through the data points. It was felt that a fractographic study of the test specimens used in the previous study[1] would help to determine the type of curve to draw through the data. This follows from the fact that all tests at 2200F were fracture tests. To this end the fracture surfaces were examined and it was found that intergranular melting began at approximately 2200F. Figures 4 - 8 show the effect of this melting on intergranular fracture. Figures 11 - 13 show the details of the grain boundary faces after fracture for the three 2200F specimens. Though all three samples were supposedly fractured at 2200F, there was apparently enough error in temperature measurement so that intergranular melting did not occur in all samples. On specimen 9, Figure 11, it is obvious that ductile tearing of the grain boundary surface occurred during fracture. This indicates that no intergranular melting occurred and that the grain boundary failed in the solid state. Specimen 15, Figure 12, shows little or no indication of ductile tearing and specimen 4, Figure 13 shows obvious melting on the grain boundary.

The fracture strains and crack analysis support the fractographic observations. Specimen 9 had no intergranular melting and supported a fracture strain of 3%. Specimen 4 had obvious melting and a fracture strain of less than 0.1%. Specimen 15 showed no ductile tearing and had a fracture strain of 0.7%. This analysis of the 2200F test data also allows for the separation of

incipient-crack strain from fracture strain for these specimens. The fracture strain and incipient-crack strain would correspond for specimen 4 because this specimen failed by a single crack growth mechanism. Specimen 15 showed a couple of cracks thus the 0.7% fracture strain did not go entirely to an incipient crack but was used to initiate several cracks. Specimen 9 showed multiple-crack grow characteristic of specimens fractured at 2175F and 2150F. Thus the observation of intergranular liquid on the grain boundary faces of specimen 4 explains the scatter in data at 2200F. This observation and its analysis also allows Figure 18 to be revised as in Figure 19 to give an accurate summary to the incipient-crack and fracture strains as a function of temperature.

Figure 19 gives an accurate account of the incipient-crack strain which would be associated with microfissuring for use in calculating microfissuring envelopes. However, as already mentioned, the strain data was taken from an on-heating type test while microfissuring is an on-cooling event. Thus the data of Figure 19 does not translate into accurate microfissuring data because the temperature axis will move to the left for on-cooling strain data. A method is needed which compensates for the temperature difference between on-heating and on-cooling test data exhibited in hot-ductility tests such as shown in Figure 1.

The key to understanding how to modify Figure 19 to account for on-cooling temperature behavior lies in understanding the microstructural changes which occur in the HAZ during welding. These changes are shown in Figure 15. It can be seen that an intergranular film forms from melting precipitates which have a high concentration of (Nb + Mo). (Nb and Mo are shown together because their chemical analysis peaks overlap in the EDAX analysis and they are not differentiated. However, the primary constituent is probably Nb.) As the grain boundary film solidifies on cooling the melting temperature is suppressed. The suppression of the melting point can be observed in the hot ductility test. In this test the nil-ductility temperature corresponds to the single-crack

growth mechanism of the hot tensile test. Thus the nil-ductility-temperature is approximately equal to the melting temperature on cooling. In terms of the distribution of intergranular liquid, the on-cooling nil-ductility-temperature of the hot ductility test would correspond to the incipient melting temperature of Figure 19 (point A). The incipient crack strain in both on-heating and on-cooling tests should be about the same. Thus the nil-ductility-temperature and the incipient melting point provide a means for adjusting the temperature scale of Figure 19 to correspond to the on-cooling temperature response of the HAZ.

Figure 20 shows the division of cracking regions for Inconel 718 based on the hot tensile test and corrected for the fractographic analysis involving the 2200F specimens per this study. It has been shown[1] that low incipient-crack strains are found at temperatures above the crack-closure region. This includes temperatures along the decreasing slope of the multiple crack growth region to the single crack growth (incipient melting) stage. It is this temperature region which constitutes the region of microfissuring susceptibility. The hot ductility test showed the same regions as Figure 20 between the nil-ductility-temperature and the maximum ductility. It is suggested that this temperature range of the hot ductility test can be used with the incipient-crack strain data of the hot tensile test to calculate microfissuring envelopes. Figure 21 shows Figure 19 corrected for on-cooling temperature dependence of strain.

The processing of Inconel 718 can have dramatic effects on its hot ductility response and hence probably on its microfissuring response. This can be seen for wrought, forged and cast material in E.G. Thompson's research.[3] Hence the hot ductility curves for a particular process should be consulted before calculating the microfissuring envelope.

SUMMARY

The correct temperature range over which to expect low-strain incipient cracking was determined using hot ductility test results. These corrected incipient crack data are summarized in Figure 21 for use in calculating microfissuring envelopes for Inconel 718. The precise incipient crack data for use with a particular processing procedure such as casting, forging etc. should be carefully considered since each processing method leads to different mechanical responses in the HAZ. These corrected data should be used in preference to data presented in earlier reports.[1]

RECOMMENDATIONS FOR FURTHER RESEARCH

Present and past research into the cracking behavior of Inconel 718 has resulted in the identification of several HAZ maladies. Foremost among these is the liquation of a secondary phase which is highly enriched in (Nb + Mo). This phase melts below the bulk melting temperature of Inconel 718 and wets the grain boundaries with the (Nb + Mo) enriched liquid. Further research is necessary to identify the processing cycles which lead to the formation of this phase in the pre-welded product. Research is also necessary to identify methods of dispersing this phase before welding. This could be done by pre-weld heat treatment or controlled processing. Furthermore, the detrimental effect of (Nb + Mo) enriched grain boundaries in the as welded product should be evaluated by mechanical testing.

BIBLIOGRAPHY

1. R. G. Thompson, Final Progress Report, NASA Contract # NAS8-33524, 1980
2. D. S. Duvall and W. A. Owczarski, Weld. J. 46, 1967, 423-s.
3. E. G. Thompson, Weld J. 48, 1459, 70-s.

APPENDIX A

FIGURES

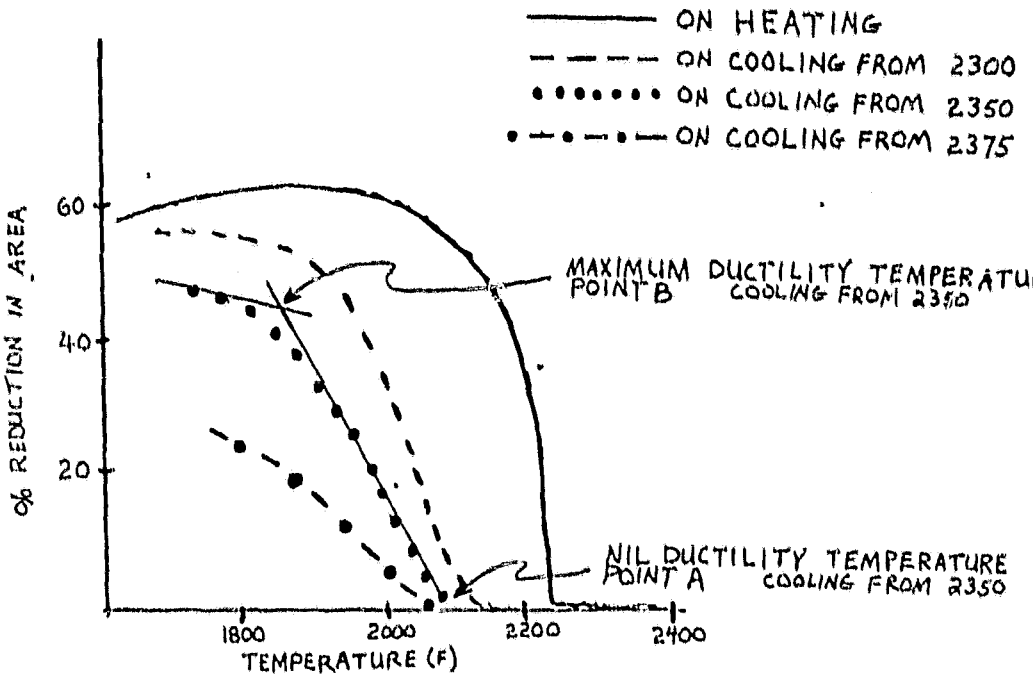

FIGURE 1 - TYPICAL HOT DUCTILITY FOR INCONEL 718. EXACT CURVE WILL VARY FROM HEAT TO HEAT AND WITH PROCESSING TECHNIQUES.

FIGURE 2 SPECIMEN 13 12X
FRACTURE TEMPERATURE 2150F
FRACTURE STRAIN 26%

FIGURE 3 SPECIMEN 14 14X
FRACTURE TEMPERATURE 2175F
FRACTURE STRAIN 11%

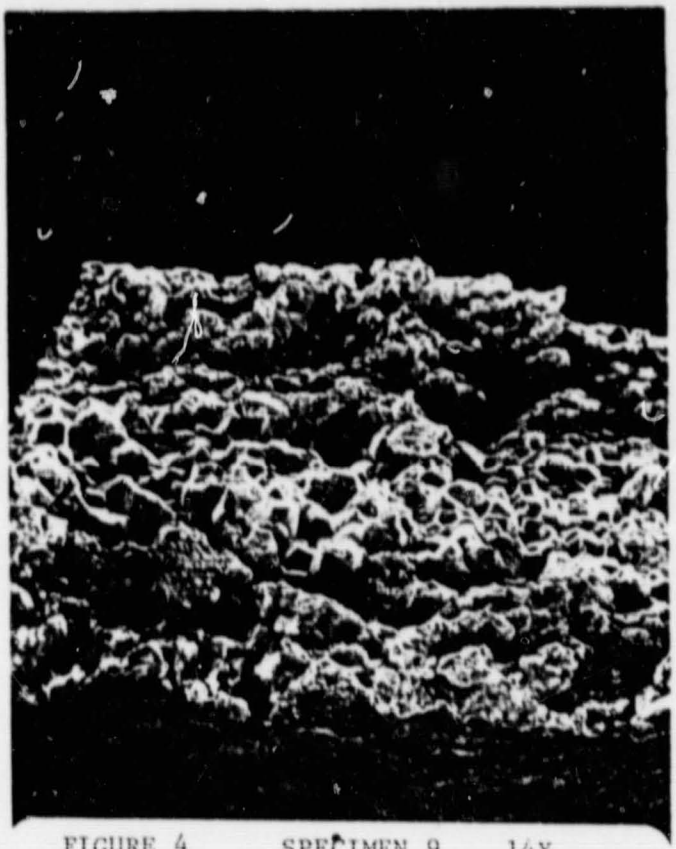

FIGURE 4 SPECIMEN 9 14X
- FRACTURE TEMPERATURE 2200F
- FRACTURE STRAIN 3%

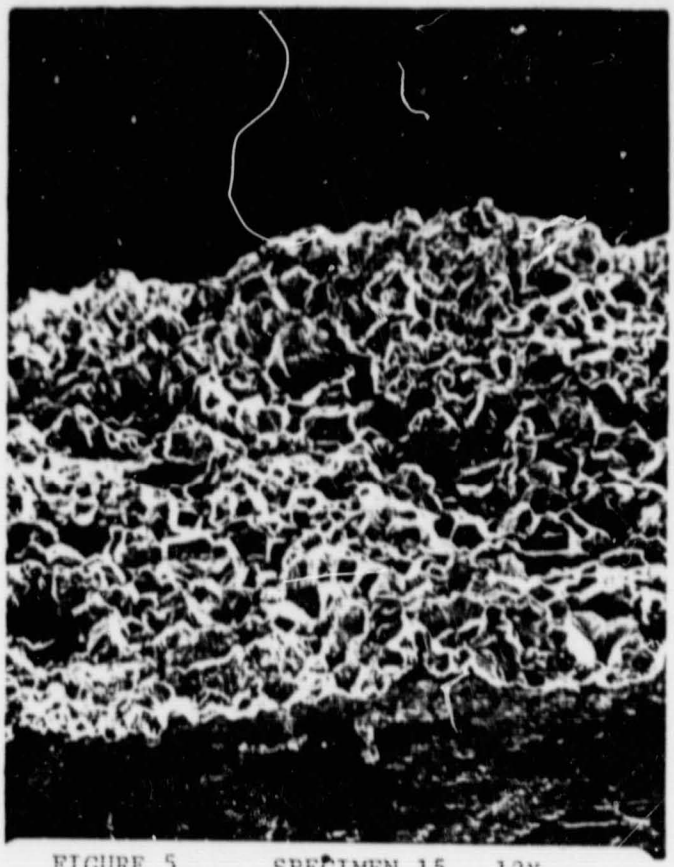

FIGURE 5 SPECIMEN 15 12X
- FRACTURE TEMPERATURE 2200F
- FRACTURE STRAIN 0.7%

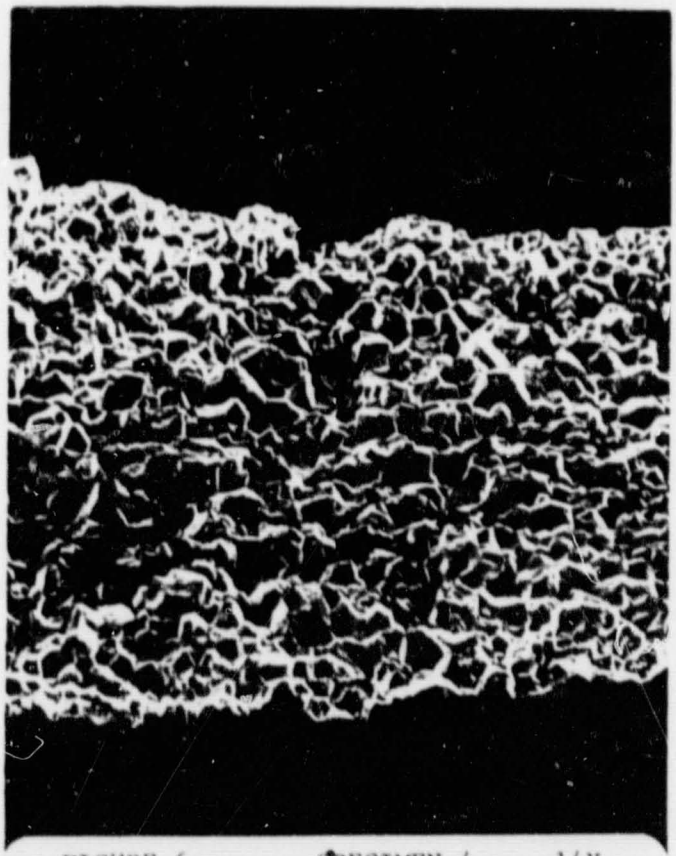

FIGURE 6 SPECIMEN 4 14X
- FRACTURE TEMPERATURE 2200F
- FRACTURE STRAIN < 0.1%

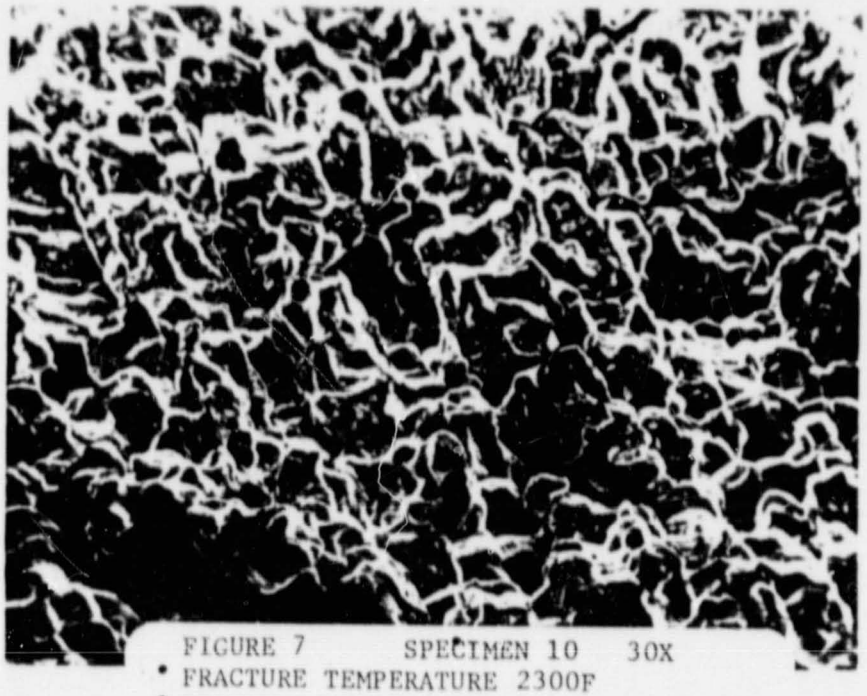

FIGURE 7 SPECIMEN 10 30X

- FRACTURE TEMPERATURE 2300F
- FRACTURE STRAIN < 0.1%

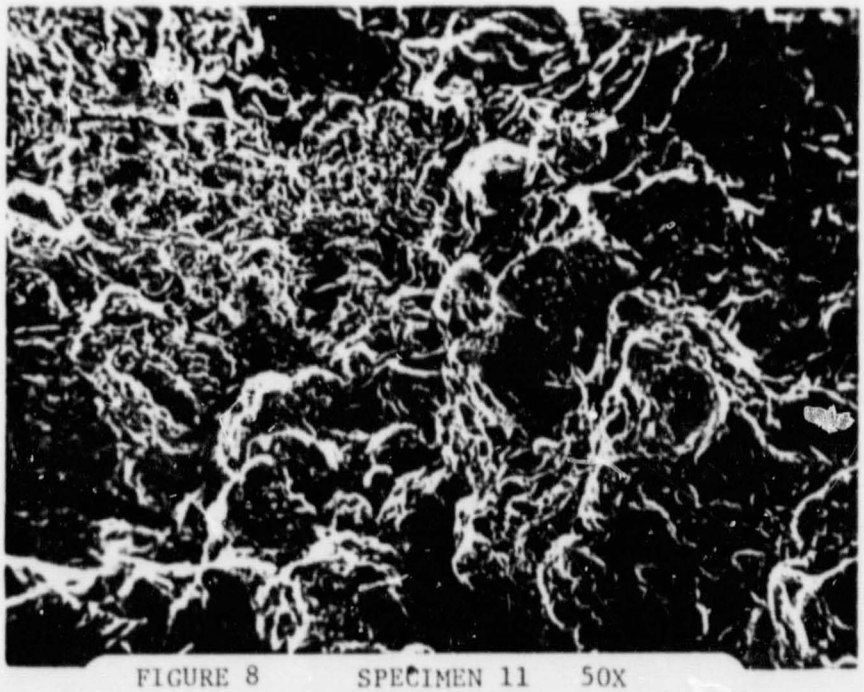

FIGURE 8 SPECIMEN 11 50X

- FRACTURE TEMPERATURE 2350F
- FRACTURE STRAIN 3%

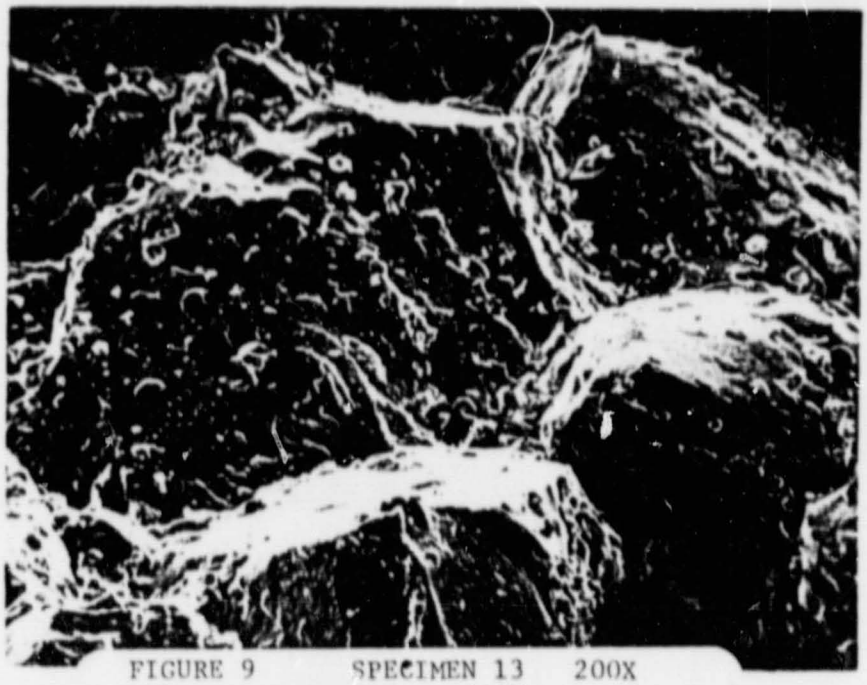

FIGURE 9 SPECIMEN 13 200X
- FRACTURE TEMPERATURE 2150F
- FRACTURE STRAIN 25%

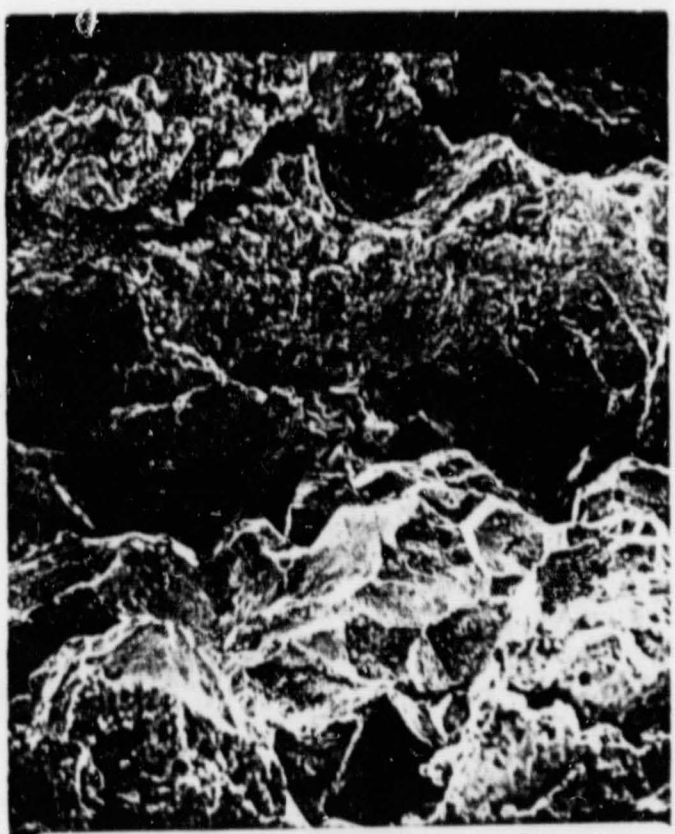

FIGURE 10 SPECIMEN 14 52X
- FRACTURE TEMPERATURE 2175F
- FRACTURE STRAIN 11%

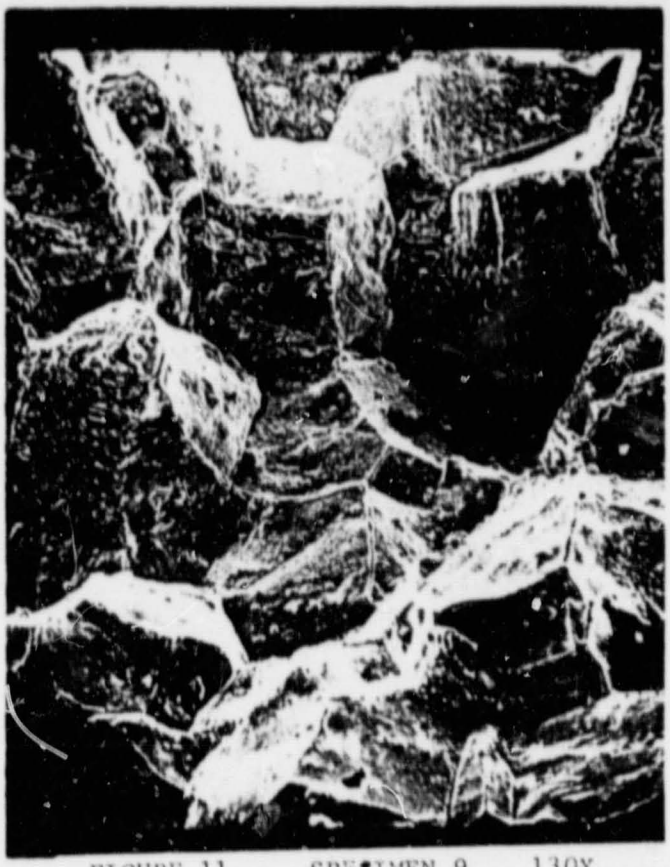

FIGURE 11 SPECIMEN 9 130X
- FRACTURE TEMPERATURE 2200F
- FRACTURE STRAIN 3%
-

FIGURE 12 SPECIMEN 15 200X
- FRACTURE TEMPERATURE 2200F
- FRACTURE STRAIN 0.7%
-

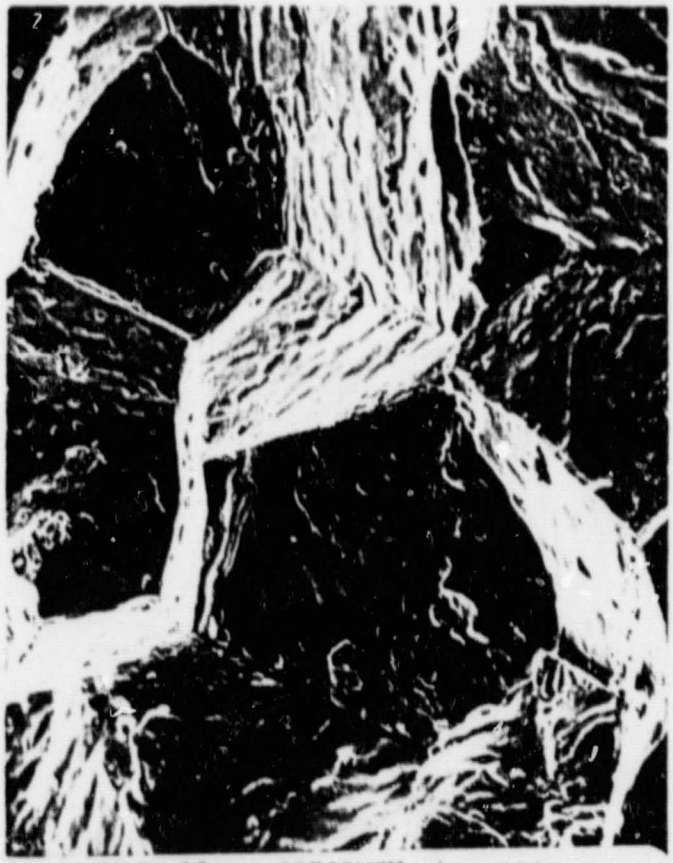

FIGURE 13 SPECIMEN 4 200X
- FRACTURE TEMPERATURE 2200F
- FRACTURE STRAIN < 0.1%
-

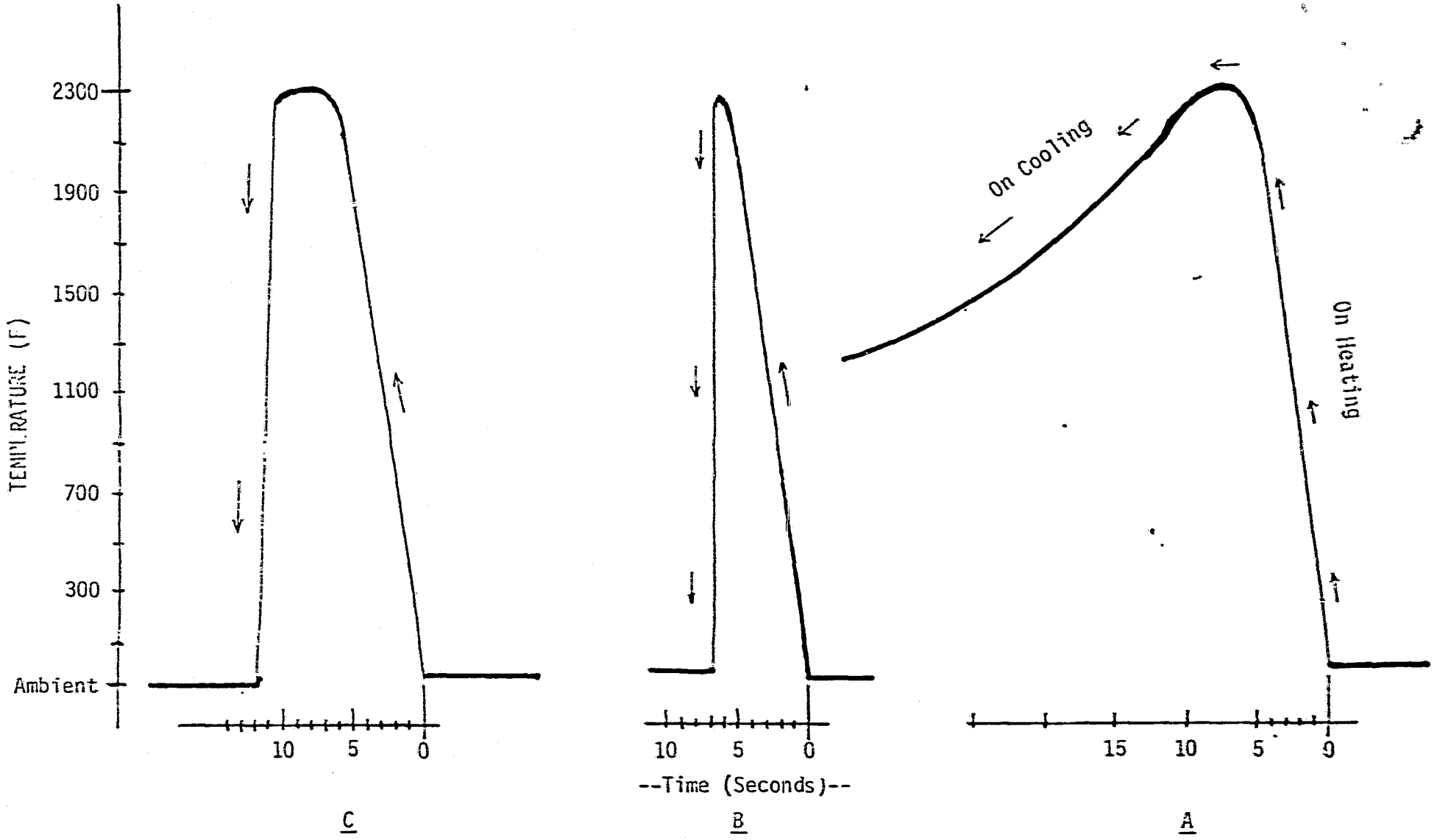

FIGURE 14- SIMULATED HAZ THERMAL CYCLE AND RAPID QUENCH RESULTS.

A. SIMULATED HAZ THERMAL CYCLE.
B. QUENCH FROM 2250 ON HEATING.
C. QUENCH FROM 2250 ON COOLING.

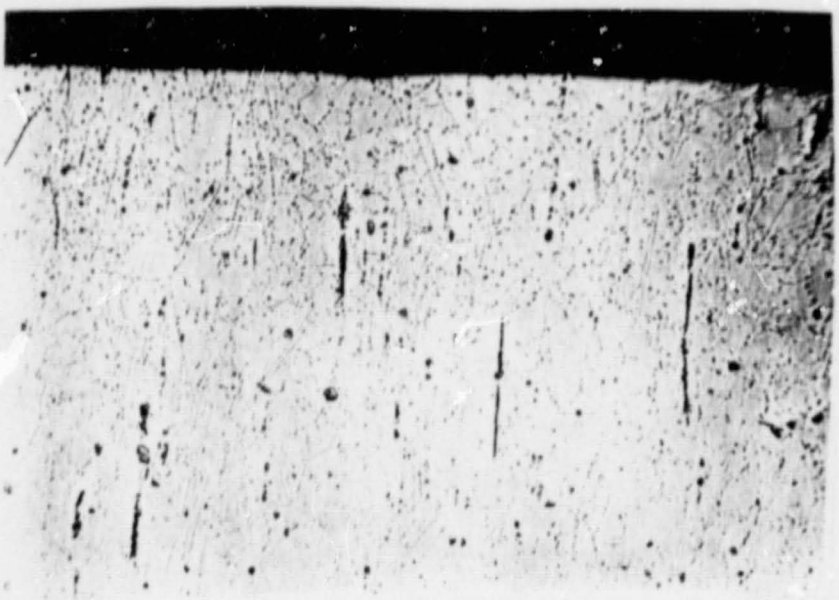

HAZ AT 2180F on HEATING; 200X

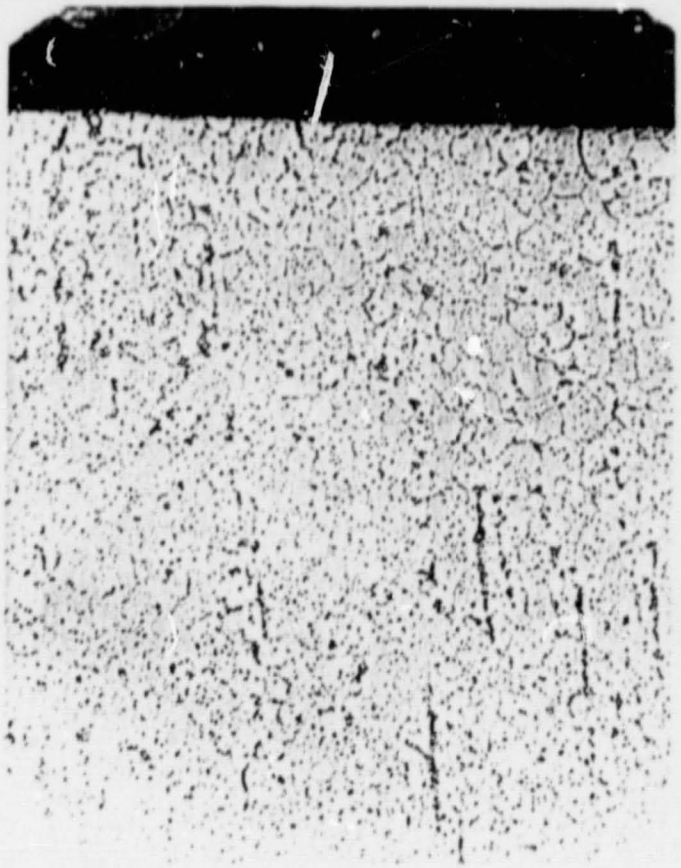

HAZ AT 2275F ON HEATING; 200X

HAZ AT 2300F MAXIMUM TEMPERATURE;
200X

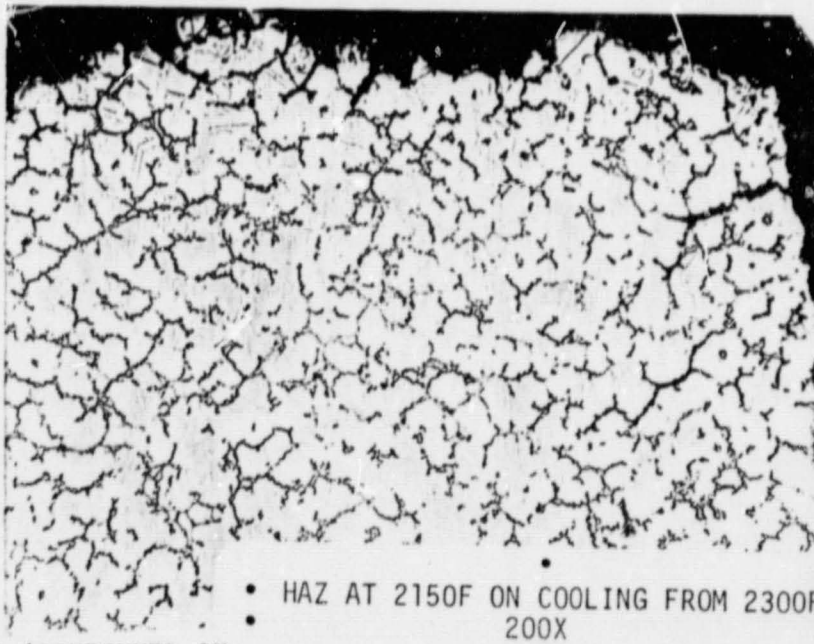

HAZ AT 2150F ON COOLING FROM 2300F
200X

FIGURE 15 (CONTINUED ON
NEXT PAGE)

Evolution of intergranular microstructure
in HAZ of Inconel 718 during a simulated

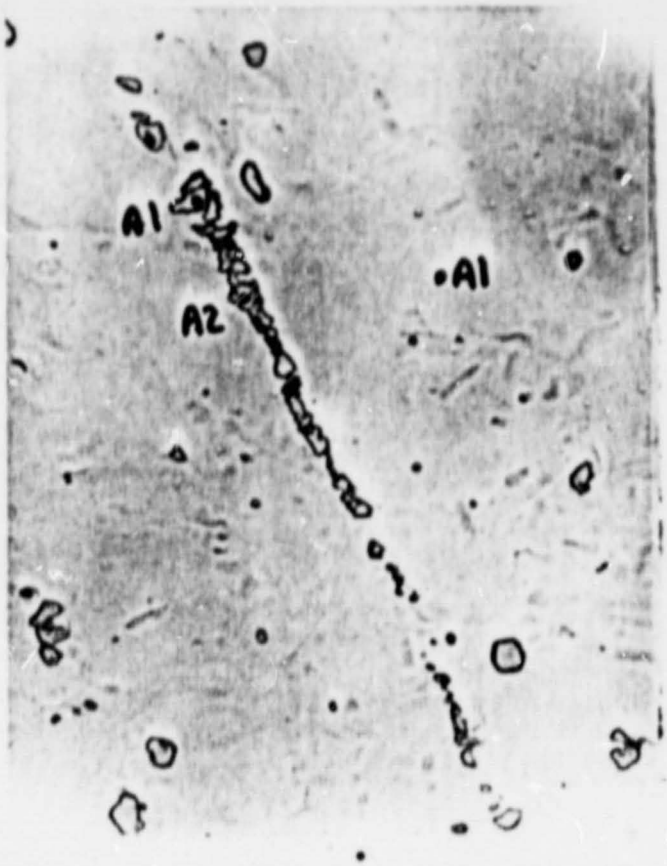

HAZ AT 2180F ON HEATING; 1200X

HAZ AT 2275F ON HEATING; 1200X

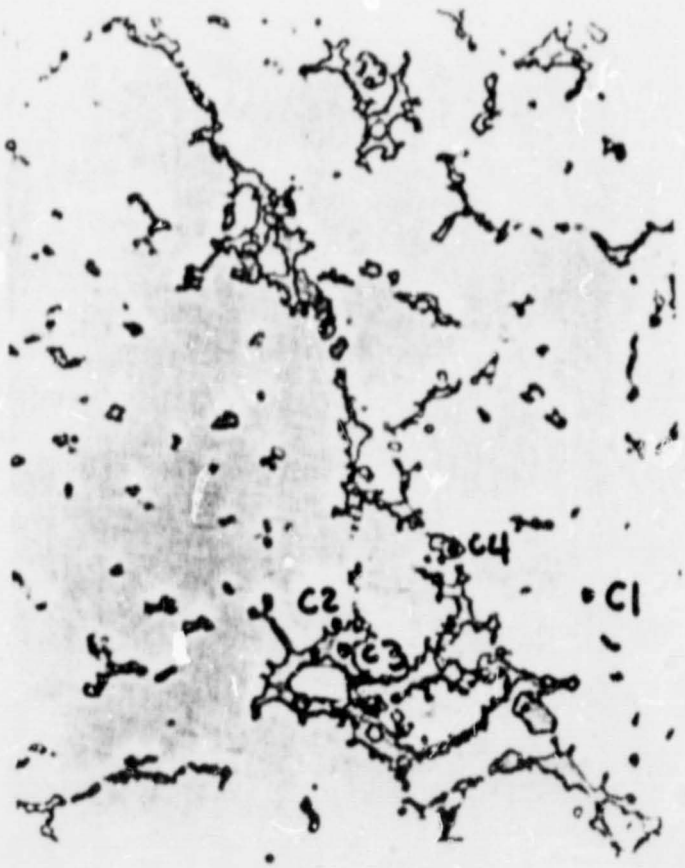

HAZ AT 2300F MAXIMUM TEMPERATURE; 1200X

HAZ AT 2150F ON COOLING FROM 2300 1200X

FIGURE 15 (CONTINUED)

FIGURE 16 EDAX ANALYSIS OF MICROSTRUCTURE

SPOT # from Figure 15	Nb	Mo	Ti	Ni	Cr	Fe	Al
A1, B1, C1, D1, B2, C2	4.8	4.3	1.1	53.0	17.5	17.9	0.8
A2, A3	36.7	10.7	3.5	26.1	10.1	9.7	2.8
B3, C3, D2	21.2	7.3	2.2	42.0	12.9	11.6	2.3
B4	64.6	12.2	8.9	5.0	2.2	1.9	4.8
C4	15.3	6.9	57.6	8.9	4.8	4.0	3.5

WET CHEMICAL ANALYSIS OF INCONEL 718

Al	Fe	Cr	Mn	Mo	Ni	V	Ti	Nb	Co	C	S
0.31	13.01	18.47	0.23	3.29	57.0	0.27	0.91	5.12	1.51	0.06	0.003

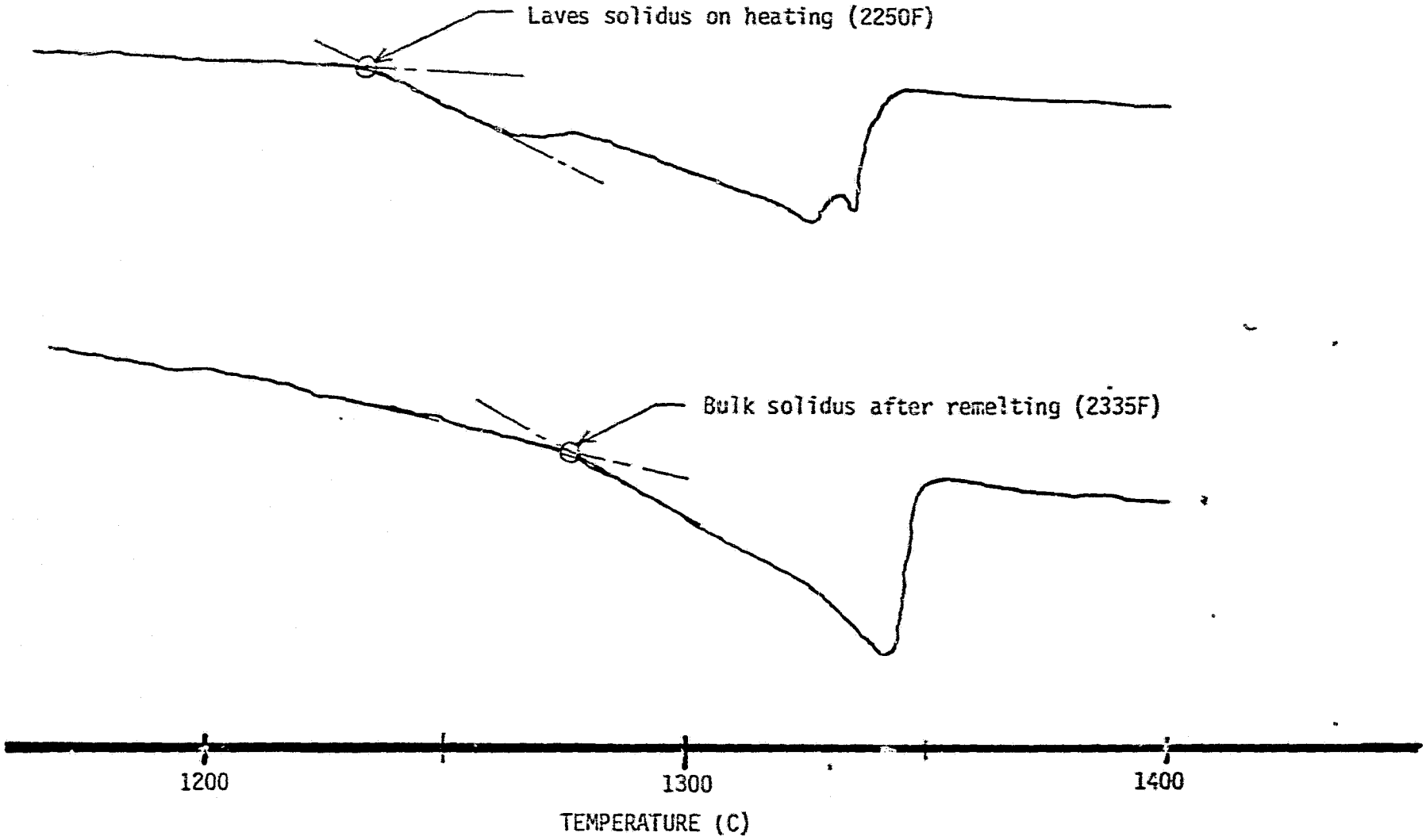

FIGURE 17 - DTA OF INCONEL 718 SHOWING SOLIDUS WITH AND WITHOUT LAVES PHASE PRESENT.

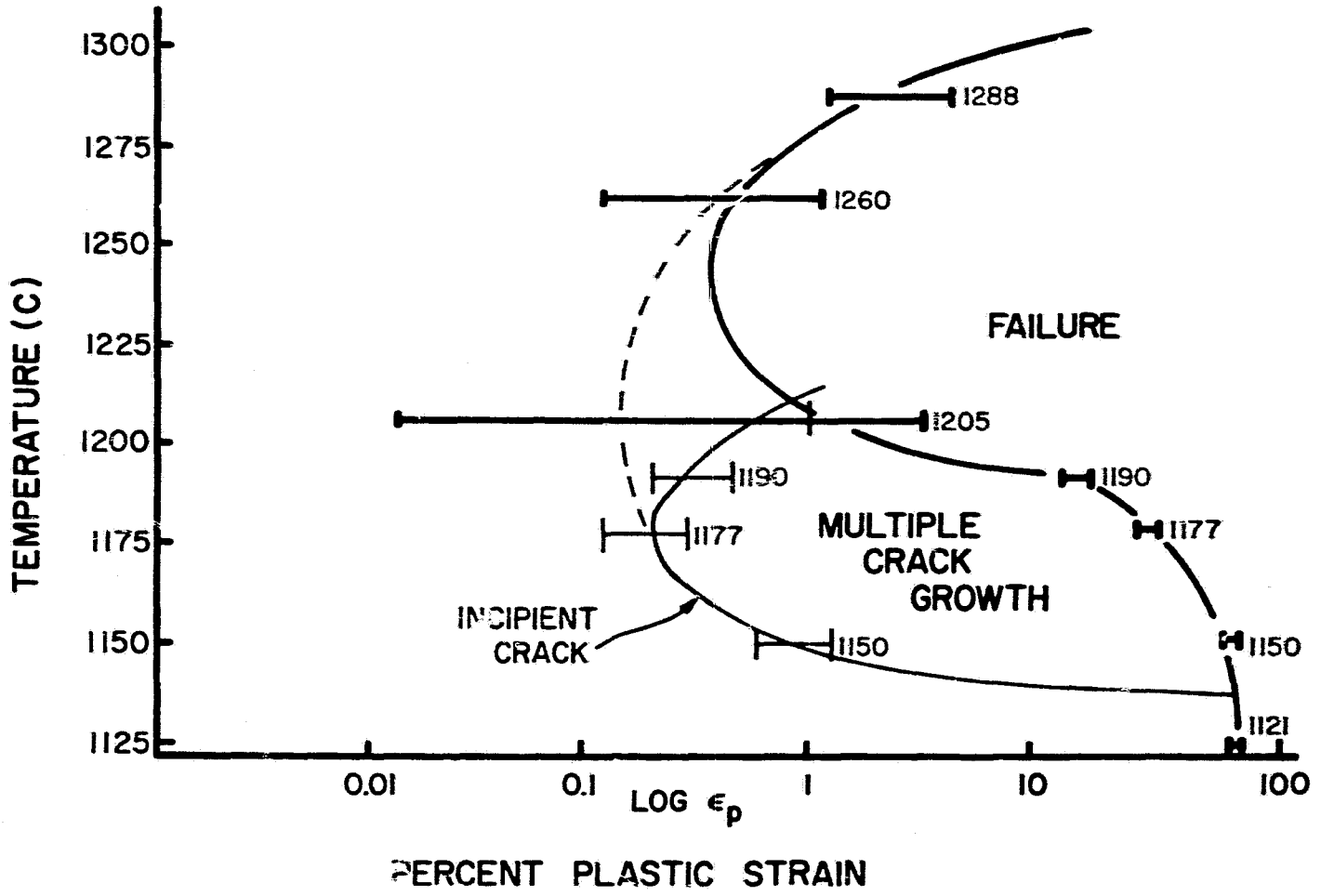

FIGURE 18 Incipient-crack stram versus temperature from previous study.[1]

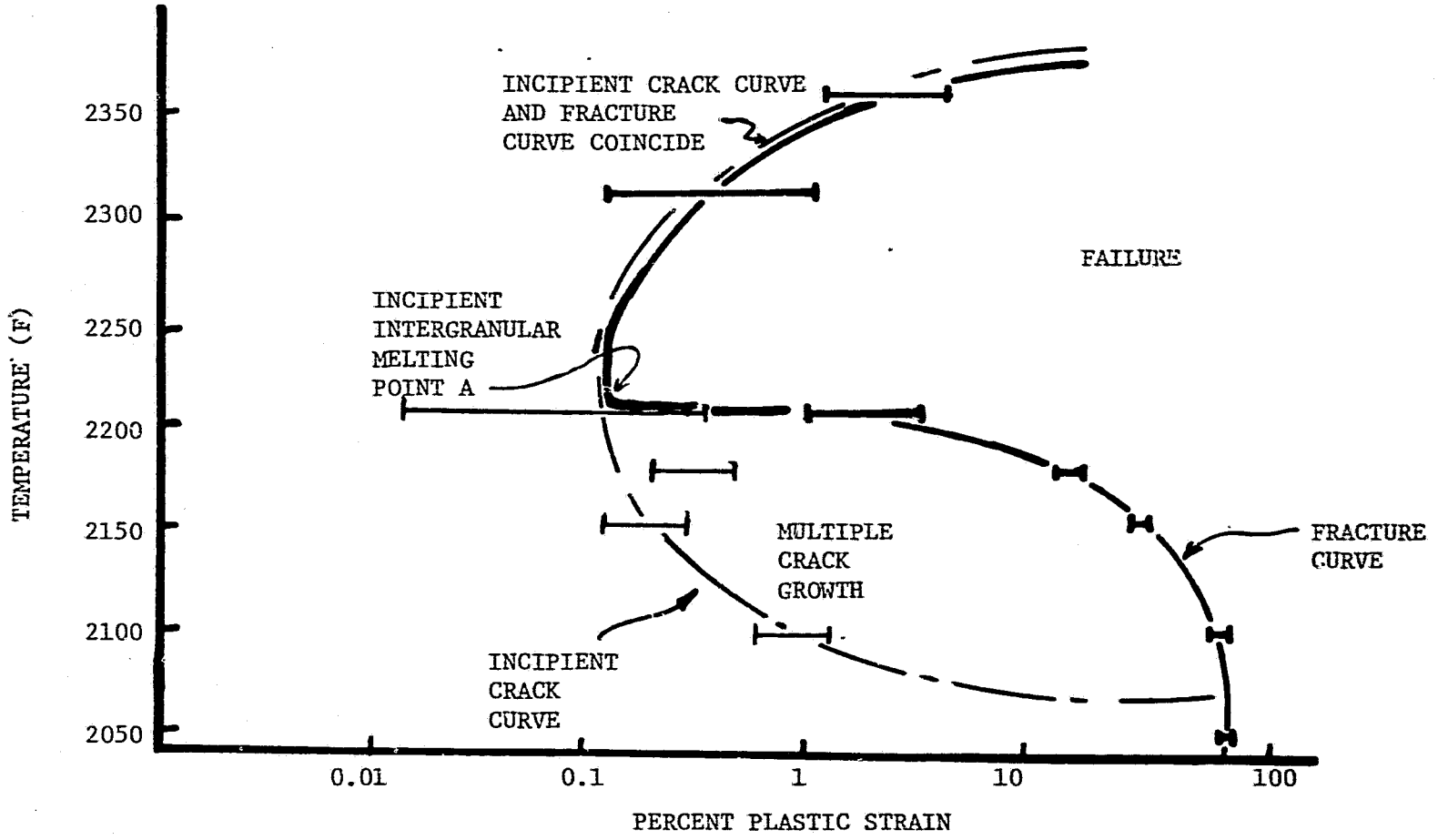

FIGURE 19. Summary of the temperature dependence of incipient-crack and fracture strains for Inconel 718. Corrected hot tensile test results,

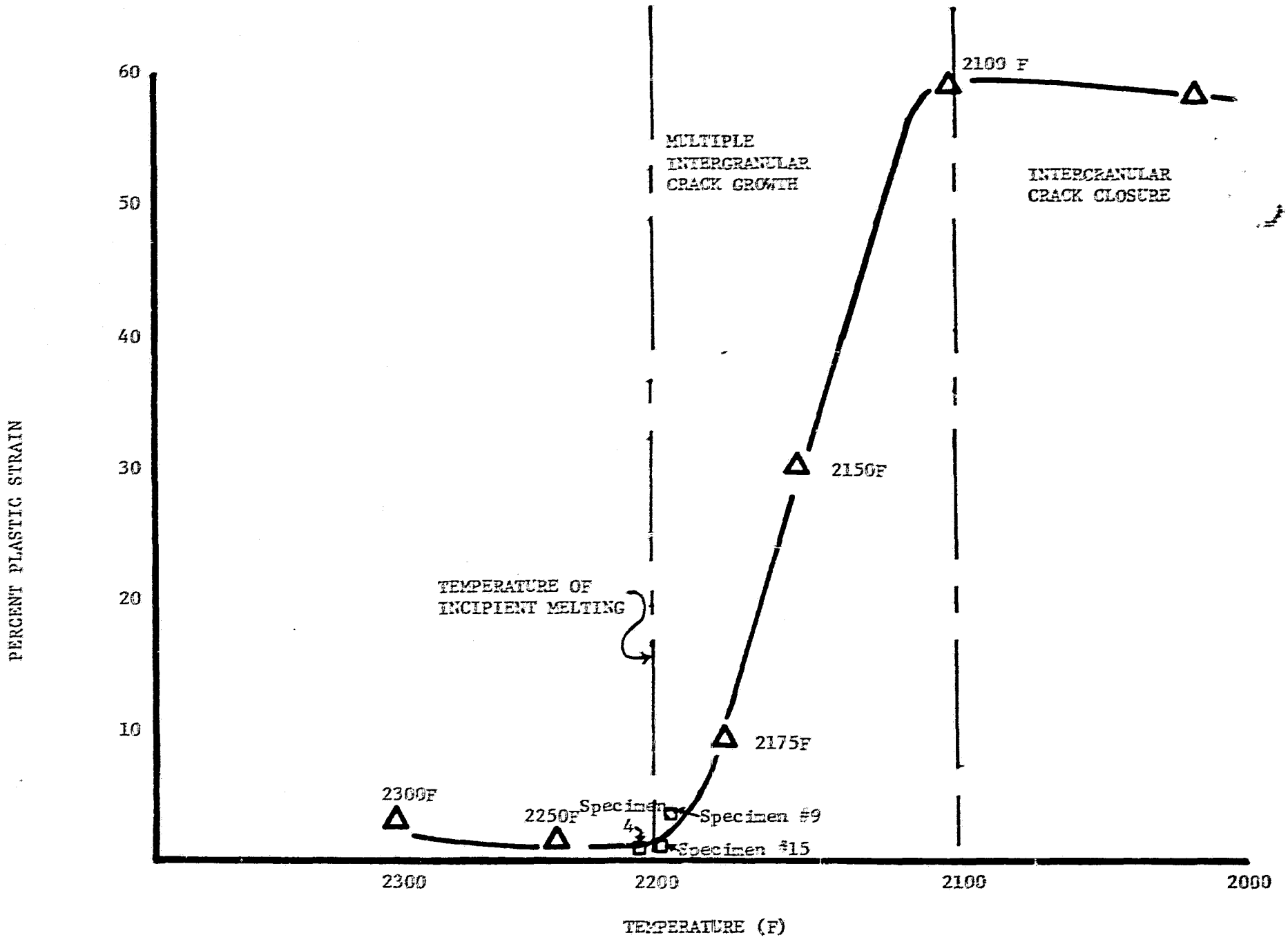

FIGURE 20, Temperature range of low-strain incipient cracking in Inconel 718 between 2100 and 2300F. Results from hot tensile test.

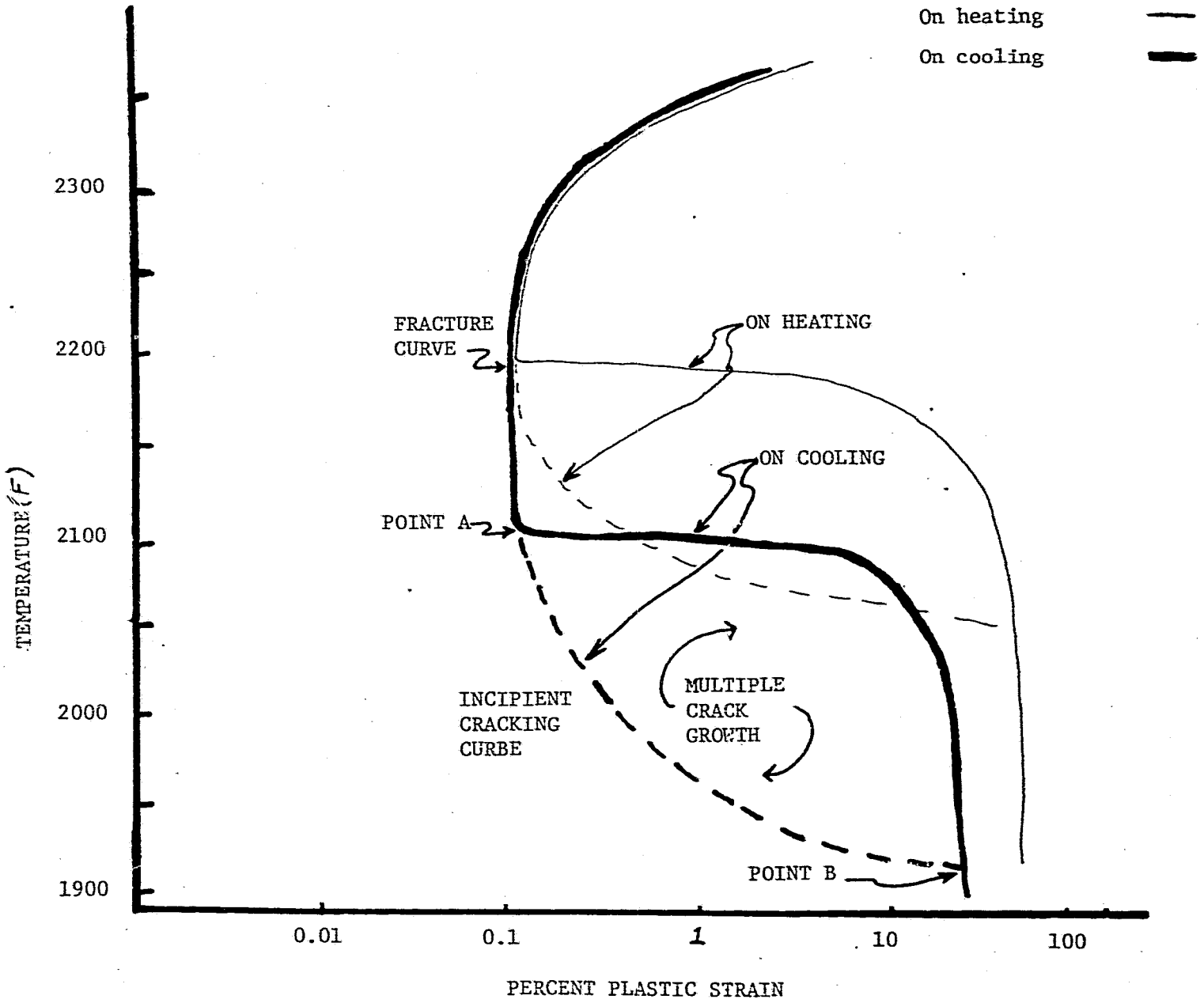

FIGURE 21 Summary of the temperature dependence of incipient crack and fracture strains for Inconel 718. Temperature dependence of strains has been adjusted by setting point A to the nil-ductility temperature and point B to the maximum strength temperature for on cooling hot ductility test. The above data is for cooling wrought Inconel 718 from a maximum temperature of 2350F.[2]